J. Fluid Mech. (1996), *vol.* 325, *pp.* 145–161

On vortex/wave interactions. Part 2. Originating from axisymmetric flow with swirl

By T. ALLEN, S. N. BROWN AND F. T. SMITH
Department of Mathematics, University College, Gower Street, London WC1E 6BT, UK

(Received 5 September 1994 and in revised form 25 April 1996)

Following the study in Part 1 of cross-flow and other non-symmetric effects on vortex/wave interactions in boundary layers, the present Part 2 applies the ideas of Part 1 and related works to an incident axisymmetric flow supplemented by a small swirl or azimuthal velocity. This is with a view to possibly increasing understanding of vortex breakdown. The wave components involved are predominantly inviscid Rayleigh-like ones. The presence of the swirl leads to extra features and complications associated mainly with extra logarithmic contributions but for the dominant interactions essentially the same equations as in Part 1 are found. These dominant nonlinear interactions must be based on azimuthal wavenumbers of ± 1 in the case of the Squire jet with swirl. In contrast to Part 1, which consisted mainly of an analysis of the quasi-bounded solutions, a representative set of numerical solutions of the full integro-differential amplitude equations is presented, for realistic axial and swirl velocity profiles. The work points also to the influence of further increases in the incident swirl.

1. Introduction

In Part 1 (Brown & Smith 1996) we studied the influences of cross-flow, and non-symmetrical input, on the nonlinear interaction between inviscid Rayleigh waves and induced streamwise vortices in an otherwise planar boundary layer. The vortex/wave interaction involved there stems from that in Smith, Brown & Brown (1993, referred to herein as SBB), again for a boundary layer.

The present Part 2 essentially asks whether the ideas on vortex/wave interaction in SBB and Part 1 can also be applied to *swirling* streamwise-vortex flows. Thus we consider the influence of an additional swirl or azimuthal velocity component on the incident motion which consists of an otherwise axisymmetric jet, say, or similar flow. The work is motivated by the long-term need for increased nonlinear studies aimed at understanding more about the phenomenon of vortex breakdown in aerodynamics and geophysical fluid flows, cf. the studies of Leibovich & Stewartson (1983), Foster & Smith (1988), Duck (1986), Brown, Leibovich & Yang (1990) and others.

The interaction of a single helical Rayleigh wave and an axisymmetric, but non-swirling, flow has recently been considered (independently) by Churilov & Shukhman (1994). Here we specify, in addition, non-symmetric input and a small swirl in the basic jet flow which is taken to be in the x-direction. The main x-velocity profile is neutrally stable to inviscid Rayleigh-like disturbances at some station $x = x_0$, around which our interest centres. Here (x, r, θ) are cylindrical polar coordinates, x, r being non-dimensionalized on the typical development length of the jet, and the corresponding velocity is (u, v, w) non-dimensionalized on the typical jet speed. The global Reynolds

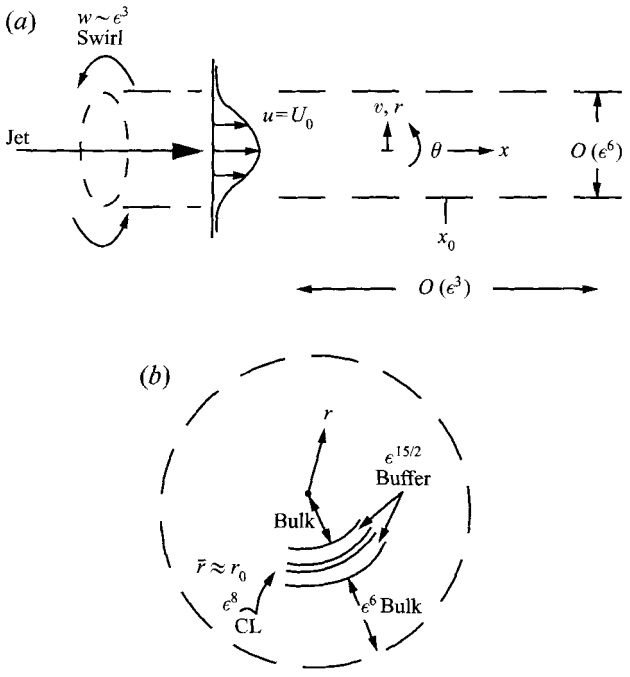

FIGURE 1. Schematic diagram of (*a*) the configuration and flow structure of an incident jet with $O(\epsilon^3)$ swirl velocities, near $x = x_0$, (*b*) the cross-sectional structure and radial scales showing the bulk (see §2), the buffer (§3) and the critical layer CL (§4).

number Re is large and is written as ϵ^{-12} for convenience. This study of the initiation of three-dimensional nonlinear interactions near x_0 is based on Part 1 and SBB, and, as in effect it is seeking to highlight any differences from, as well as similarities to, the vortex/wave interaction balances in those papers due to the current incident axisymmetry and rotation, e.g. differences due to centrifugal forces, not all the details need to be followed through. The Navier–Stokes equations, which read

$$u_x + v_r + r^{-1}(v + w_\theta) = 0, \tag{1.1}$$

$$\mathcal{N}(u) \equiv (\partial_t + u\partial_x + v\partial_r + r^{-1}w\partial_\theta)u = -p_x + \epsilon^{12}\nabla^2 u, \tag{1.2}$$

$$\mathcal{N}(v) - r^{-1}w^2 = -p_r + \epsilon^{12}[\nabla^2 v - r^{-2}(v + 2w_\theta)], \tag{1.3}$$

$$\mathcal{N}(w) + r^{-1}vw = -r^{-1}p_\theta + \epsilon^{12}[\nabla^2 w - r^{-2}(w - 2v_\theta)], \tag{1.4}$$

with ∇^2 denoting $(\partial_x^2 + \partial_r^2 + r^{-1}\partial_r + r^{-2}\partial_\theta^2)$, are treated for small ϵ with x near x_0 and a given u-profile $U_0(\bar{r})$ and swirl (w-) profile $\epsilon^3 W_0(\bar{r})$ at x_0. The significance of the swirl velocity scaling of order ϵ^3 is analogous with that of the cross-flow in Part 1, despite some differences as we shall see, and we should remark that this $O(\epsilon^3)$ velocity, while small, is much larger than in vortex/wave interactions studied prior to Part 1, apart from Davis & Smith's (1994) case of a vortex/wave interaction incorporating viscous Tollmien–Schlichting-like waves with cross-flow. Here also $r = \epsilon^6 \bar{r}$ with $\bar{r}$ of order unity for the most part since the input jet or other axisymmetric oncoming flow has typical thickness of $O(\epsilon^6)$, e.g. Squire's form $U_0 \propto (\bar{r}^2 + \bar{a}^2)^{-2}$ (for constant $\bar{a}$) which is an exact solution of the axisymmetric jet equations. Incidentally Foster & Smith (1988) note the relation between Long's vortex and the Squire profile (see also Burggraf & Foster 1977), while Batchelor & Gill (1962) suggest that the latter profile is neutrally stable for

an azimuthal wavenumber of unity, a result verified in this work. As in Part 1 two streamwise scales operate: $x-x_0 = \epsilon^3 x_1$ and $\epsilon^6 X$ with a corresponding fast time scale $t = \epsilon^6 T$. The inviscid wave that starts near $x = x_0$ is dependent on both the fast (X, T) and the slow (x_1) scales, the latter being associated with initially slow growth/non-neutrality, whereas the three-dimensional vortex is independent of the fast scales. Typically a fixed frequency Ω close to the neutral value Ω_0 is assumed, and/or wavenumber and wave speed α, c or position x close to α_0, c_0, x_0.

The scales and flow structure involved are essentially as in Part 1 and SBB but for the nearly axisymmetric setting (figure 1). The added swirl effect however produces a more singular wave response (§2) than in Part 1, at the critical layer, as well as extra logarithmic contributions and powers thereof, and these require some detailed description (§§3, 4). Despite these and other complications the governing amplitude equations of the vortex/wave interaction turn out to be virtually the same as in Part 1 for cross-flow effects. In §5 we present numerical solutions of the full integro-differential amplitude equations for the Squire jet combined with a Batchelor vortex for the swirl profile and variations thereon. These embrace all possible downstream behaviours in contrast to the study in Part 1 which was restricted in the main to an analysis of the quasi-bounded solutions only. The present study is helpful also in showing the explicit appearance of the various swirl effects particularly in the buffer and critical-layer regions of §§3, 4, in readiness for analysis on increased swirl. Further comments are presented in §6.

2. The bulk

The main bulk or core of the motion, as shown in the flow structure of figure 1, has $r \equiv \epsilon^6 \bar{r}$ with $\bar{r}$ and θ of $O(1)$ throughout. The flow-field solution expands in the underlying form

$$u = U_0(\bar{r}) + \epsilon^3 U_1(x_1, \bar{r}) + \ldots + \epsilon^{m-3} U_3(x_1, \bar{r}, \theta) + \ldots + E[\epsilon^7 u^{(0)} + \epsilon^{10} u^{(1)} + \ldots] + \text{c.c.} + \ldots, \quad (2.1)$$

$$v = \epsilon^6 V_1(\bar{r}) + \epsilon^9 V_2(x_1, \bar{r}) + \ldots + \epsilon^m V_3(x_1, \bar{r}, \theta) + \ldots + E[\epsilon^7 v^{(0)} + \epsilon^{10} v^{(1)} + \ldots] + \text{c.c.} + \ldots, \quad (2.2)$$

$$w = \epsilon^3 W_0(\bar{r}) + \epsilon^6 W_2(x_1, \bar{r}) + \ldots + \epsilon^m W_3(x_1, \bar{r}, \theta) + \ldots + E[\epsilon^7 w^{(0)} + \epsilon^{10} w^{(1)} + \ldots] + \text{c.c.} + \ldots, \quad (2.3)$$

$$p = p_{00} + \ldots + \epsilon^6 Q_0(\bar{r}) + \epsilon^9 Q_1(\bar{r}) x_1 + \ldots + \epsilon^{12} q_{12} + \ldots + E[\epsilon^7 p^{(0)} + \epsilon^{10} p^{(1)} + \ldots] + \text{c.c.} + \ldots, \quad (2.4)$$

where c.c. denotes the complex conjugate of the preceding expression, U_0 is the incident axial velocity profile, e.g. Squire's form, and $\epsilon^3 W_0$ denotes the added incident swirl. The order of magnitude, $O(\epsilon^3)$, of the imposed incident swirl here is exactly that of the imposed cross-flow in Part 1. The power m controlling the non-symmetric parts of the mean flow here is to be determined by matching with the buffer zone, U_k, V_k, W_k are mean-flow components, and $u^{(k)}, v^{(k)}, w^{(k)}, p^{(k)}$ are successive wave components. These components are proportional to $E \equiv \exp[\mathrm{i}(\alpha X - \Omega T)]$, which is to stay neutral with wavenumber $\alpha \approx \alpha_0 + \epsilon^3 \alpha_2 x_1$, wave speed $c = \Omega/\alpha \approx c_0 + \epsilon^3 c_2 x_1$. Below, we examine the mean flow, which is mostly axisymmetric but with a small non-symmetric vortex component, in §2.1, followed by the non-symmetric wave components in §2.2. In both cases the bulk properties are predominantly inviscid.

2.1. *The mean flow*

The balances of continuity and (x, r, θ) momentum from substitution of (2.1)–(2.4) into (1.1)–(1.4) are to leading order

$$U_{1x_1} + V_{1\bar{r}} + \bar{r}^{-1} V_1 = 0, \tag{2.5}$$

$$U_0 U_{1x_1} + V_1 U_0' = U_0'' + \bar{r}^{-1} U_0', \tag{2.6}$$

$$-\bar{r}^{-1} W_0^2 = -Q_0', \tag{2.7}$$

$$U_0 W_{2x_1} + V_1 W_0' + \bar{r}^{-1} V_1 W_0 = W_0'' + \bar{r}^{-1} W_0' - \bar{r}^{-2} W_0, \tag{2.8}$$

provided $m > 6$. These control the mean-flow terms $U_1(\propto x_1)$, V_1 from (2.5), (2.6) and W_2 from (2.8), with (2.7) showing the mean centrifugal force–swirl balance. The next-order equations then govern the mean-flow terms U_2, V_2 and so on, depending on the value of m; later analysis fixes m to be 9, which confirms the negligible role of the non-symmetric vortex components in the present bulk flow.

The input axial profile is assumed to be smooth (with say $U_0(\infty)$ zero, $U_0(0)$ non-zero, $U_0'(0)$ zero) and neutrally stable. In what follows we are interested for example in the flow behaviour near the critical radius $\bar{r} = r_0$ at which $U_0 = c_0$; so there

$$U_0 \sim c_0 + \sum_1^\infty \Gamma_k s^k \tag{2.9}$$

is regular, the Γ_k being constants, and $s \equiv \bar{r} - r_0$. The shear and curvature values Γ_1, Γ_2 here are inter-related only via the wavenumber α_0 in effect, as found in §2.2. The input swirl profile has $W_0 \sim \delta_0 + s\delta_{01}$ as $\bar{r} \to r_0$ where δ_0, δ_{01} are constants.

2.2. *The wave components*

Working to higher order to obtain the E components, we find that the two dominant pressure parts satisfy the free and forced Rayleigh inviscid-wave equations

$$\mathscr{L}_0(p^{(0)}) \equiv p^{(0)}_{\bar{r}\bar{r}} + \left[\frac{1}{\bar{r}} - \frac{2U_0'}{(U_0 - c_0)}\right] p^{(0)}_{\bar{r}} + \frac{p^{(0)}_{\theta\theta}}{\bar{r}^2} - \alpha_0^2 p^{(0)} = 0, \tag{2.10}$$

$$\mathscr{L}_0(p^{(1)}) = \Delta u^{(0)}_{x_1} + \mathrm{i}\alpha_0 R_2 - 2\mathrm{i}\alpha_0 U_0' \Delta^{-1} R_3 + \bar{r}^{-1}[(\bar{r}R_3)_{\bar{r}} + R_{4\theta}], \tag{2.11}$$

respectively. Hence $\Delta \equiv \mathrm{i}\alpha_0(U_0 - c_0)$, and

$$R_2 \equiv \mathrm{i}\Omega_2 u^{(0)} - U_0 u^{(0)}_{x_1} - \mathrm{i}\alpha_0 U_1 u^{(0)} - v^{(0)} U_{1\bar{r}} - \bar{r}^{-1} W_0 u^{(0)}_\theta - p^{(0)}_{x_1}, \tag{2.12}$$

$$R_3 \equiv \mathrm{i}\Omega_2 v^{(0)} - U_0 v^{(0)}_{x_1} - \mathrm{i}\alpha_0 U_1 v^{(0)} - \bar{r}^{-1} W_0 (v^{(0)}_\theta - 2w^{(0)}), \tag{2.13}$$

$$R_4 \equiv \mathrm{i}\Omega_2 w^{(0)} - U_0 w^{(0)}_{x_1} - \mathrm{i}\alpha_0 U_1 w^{(0)} - v^{(0)} W_0' - \bar{r}^{-1} W_0 (w^{(0)}_\theta + v^{(0)}), \tag{2.14}$$

containing the influences of swirl, non-parallelism, modulation and frequency shift. Depending on how the input frequency is fixed the shift Ω_2 may be zero or non-zero, and similar allowances are assumed for the wavenumber and wave-speed shifts α_2, c_2. Also,

$$u^{(0)} = -(\mathrm{i}\alpha_0 p^{(0)} + U_0' v^{(0)})/\Delta, \quad v^{(0)} = -p^{(0)}_{\bar{r}}/\Delta, \quad w^{(0)} = -p^{(0)}_\theta/(\bar{r}\Delta), \tag{2.15}$$

$$u^{(1)} = (R_2 - \mathrm{i}\alpha_0 p^{(1)} - U_0' v^{(1)})/\Delta, \quad v^{(1)} = (R_3 - p^{(1)}_{\bar{r}})/\Delta, \quad w^{(1)} = \left(R_4 - \frac{p^{(1)}_\theta}{\bar{r}}\right)/\Delta \tag{2.16}$$

give the velocity components.

Hence the main, neutral, wave has $p^{(0)} = (r_+ \hat{e} + r_- \hat{e}^{-1}) P_0(\bar{r})$ say, with $\hat{e} \equiv \exp(\mathrm{i}n\theta)$, integer n (see figure 2), and $r_\pm$ independent of $\bar{r}, \theta$, yielding for the subsequent part

$p^{(1)} \ni \hat{e}^{\pm 1} P_0 Q^{(1)}$ say for its $\hat{e}^{\pm 1}$ contributions. To these can be added multiples of $p^{(0)}$. Here $Q^{(1)}(\bar{r}, x_1)$ satisfies, from (2.11),

$$P_0^2 \bar{r}\gamma^{-2} Q_{\bar{r}}^{(1)} = \int_{\infty}^{\bar{r}} \frac{\hat{r} P_0}{\gamma^3} \{r_+(x_1)\,(\mathrm{RHS})_a + \mathrm{i}c_0\, r'_+(x_1)\,(\mathrm{RHS})_b + \sigma r_+(x_1)\,(\mathrm{RHS})_c\}\,\mathrm{d}\hat{r}, \quad (2.17)$$

for the r_+ part. This applies in $\bar{r} > r_0$, where $\gamma \equiv U_0 - c_0$ vanishes at r_0, while the terms on the right-hand side are

$$(\mathrm{RHS})_a = 2P_0'(U_{1\bar{r}} - (U_1 - \Omega_2/\alpha_0)\, U_0' \gamma^{-1}), \quad (2.18)$$

$$(\mathrm{RHS})_b = 2\alpha_0^{-1}(P_0'\, U_0' \gamma^{-1} - \alpha_0^2 P_0\, \gamma c_0^{-1}), \quad (2.19)$$

$$\sigma(\mathrm{RHS})_c = 2n\alpha_0^{-1} \left\{ \frac{P_0[3U_0' W_0 \hat{r} - \gamma(\hat{r}W_0' - W_0)]}{\hat{r}^3 \gamma} + \frac{P_0'[-U_0' W_0 \hat{r} + \gamma(\hat{r}W_0' - W_0)]}{\hat{r}^2 \gamma} \right\}. \quad (2.20)$$

In $0 < \bar{r} < r_0$ the integration range in (2.17) is altered to $0 < \hat{r} < \bar{r}$, cf. SBB where a wall effect is also present, while the formulae for the r_- parts here and below are analogous with those in (2.17)–(2.20) ff. The terms (2.18), (2.19) are similar to those in SBB, but (2.20) represents the extra effect due to the input swirl, the constant σ being a measure of the W_0 velocity.

What matters most now is the flow response near the critical radius, as s tends to zero. There the leading wave is regular,

$$P_0 \sim 1 + \sum_1^{\infty} q_k s^k, \quad (2.21)$$

and (2.10) in mode form combined with (2.9) requires that $q_1 = 0, 2q_2 = -\Lambda$, whereas q_3 remains arbitrary locally, consistent with the inflexion-point-like condition

$$r_0 \Gamma_1^{-1} \Gamma_2 = \tfrac{1}{2} - r_0^{-2} \Lambda^{-1} n^2, \quad (2.22)$$

where $\Lambda \equiv (\alpha_0^2 + r_0^{-2} n^2)$. A computation for the neutral solution P_0, α_0, c_0, r_0 is given in figure 2 for the case of the Squire jet (see also Batchelor & Gill 1962). To determine the subsequent-order wave we use the responses

$$\gamma^{-3} \bar{r} P_0 (\mathrm{RHS})_a \sim a_{-3} s^{-3} + a_{-2} s^{-2} + \ldots, \quad (2.23)$$

$$\gamma^{-3} \bar{r} P_0 (\mathrm{RHS})_b \sim b_{-3} s^{-3} + b_{-2} s^{-2} + \ldots, \quad (2.24)$$

from (2.18), (2.19) with (2.21), similarly to SBB, whereas (2.20) leads to the more singular response

$$\gamma^{-3} \bar{r} P_0\, \sigma(\mathrm{RHS})_c \sim \kappa_{-4} s^{-4} + \kappa_{-3} s^{-3} + \ldots. \quad (2.25)$$

The dominant term here has coefficient $\kappa_{-4} = 6n\delta_0/(r_0 \Gamma_1^3 \alpha_0)$. Thus (2.23), (2.24) yield terms analogous with SBB's (3.19), i.e. of orders $1, s, s^2, s^3 \ln|s|, s^3$ in $\hat{e}^{-1} p^{(1)}$, with a jump in the coefficient of s^3 across $\bar{r} = r_0(\pm)$. In contrast, the swirl-driven contribution (2.25) produces the terms

$$\chi_{0L} \ln|s| + \chi_0 + \chi_1 s + \chi_{2L} s^2 \ln|s| + \chi_2 s^2 + \chi_{3L} s^3 \ln|s| + \chi_3 s^3 + \ldots \quad \text{in} \quad \hat{e}^{-1} p^{(1)}. \quad (2.26)$$

Here $\chi_{0L} = -\Gamma_1^2 \kappa_{-4}/(3r_0)$ is continuous, $\chi_0^{\pm} = -\Gamma_1^2 I_2^{\pm}/(3r_0)$ is discontinuous, $\chi_{2L} = \Gamma_1^2 \Lambda \kappa_{-4}/(6r_0)$ is continuous, $\chi_2^{\pm}$ is discontinuous, and the terms χ_1, χ_2, χ_3 add to those in (3.19) of SBB. Further, $I_2^{\pm}$ denote the finite parts of integrals with respect to $\bar{r}$ from r_0 to ∞, 0 to r_0, respectively. Of the terms in (2.26), the jumps in both χ_0, χ_2 can be accommodated satisfactorily in the bulk-flow solution by adding to $\hat{e}^{-1} p^{(1)}$ different multiples of P_0 for $\bar{r} > r_0, \bar{r} < r_0$, accompanied by corresponding additions to the wave

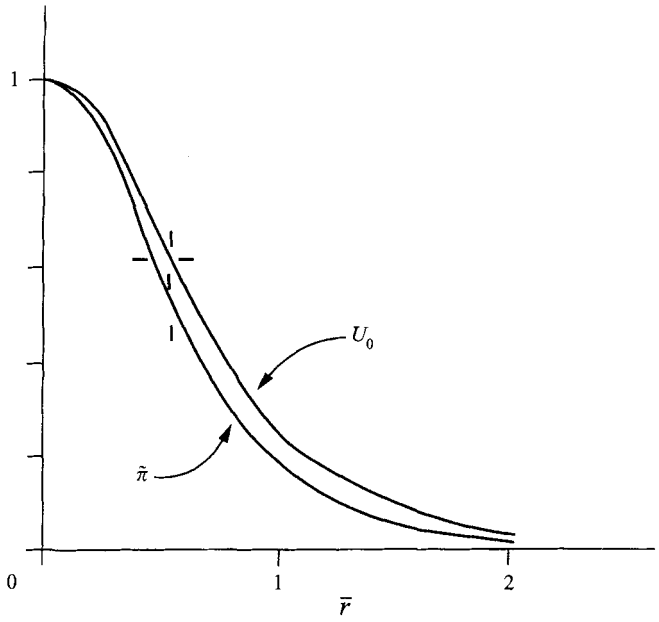

FIGURE 2. Numerical solution for the dominant wave-pressure function $\tilde{\pi}(\bar{r}) \propto P_0/\bar{r}$ when $n = 1$, in the case of the Squire-jet normalized profile $U_0 \equiv (1+\bar{r}^2)^{-2}$. The wavenumber is $\alpha_0 \approx 1.461$, while the dashed lines indicate the critical level r_0 (see (2.22)). The results are from extrapolation of the solutions obtained on grids of 501×0.02 and 1001×0.01 in $\bar{r}$. Solutions appeared to be unobtainable for $|n| \neq 1$, cf. Batchelor & Gill (1962) who showed that there are no neutral solutions for $|n| > 1$ and obtained $\alpha_0 \approx 1.46$ for $n = 1$.

velocity components. The logarithmic terms associated with χ_{0L}, χ_{2L} are found later to jump by $i\pi \operatorname{sgn} \Gamma_1$, adding to the χ_0, χ_2 jumps, these and other logarithms being smoothed out in the viscous critical layer of §4. Therefore the major influence of (2.26) is its extra jump contribution at order s^3, via $\chi_3^{\pm}$, supplementary to those in SBB's (3.19) by an amount $\sigma(G_c^+ - G_c^-)\, r(x_1)$ say. Here $G_c^+ - G_c^-$ is complex, the real part arising from $(\mathrm{RHS})_c$ in (2.20) and the imaginary part from q_3 in (2.21) in the different multiples of P_0 added to $\hat{\epsilon}^{-1}p^{(1)}$ in $\bar{r} > r_0, \bar{r} < r_0$. Other extra swirl-induced effects including logarithms [e.g. $v^{(1)} \propto \ln|s|$ due to (2.26)] are also present but discussion of them is best deferred until §4. Likewise, higher-order effects such as in the induced E^2 nonlinear terms play a negligible role at this stage. We turn next to the buffer- and critical-layer responses.

3. The buffer

This zone lying astride the critical layer is associated mostly with viscous–inviscid changes in the mean vortex components. The buffer has $r = \epsilon^6(r_0 + \epsilon^{3/2} Y_1)$ with Y_1 of order unity, so that $s \to \epsilon^{3/2} Y_1$ formally, and on account of (2.1)–(2.4) ff. the appropriate expansion is

$$u = c_0 + \epsilon^{3/2}\Gamma_1 Y_1 + \epsilon^3(\Gamma_2 Y_1^2 + c_2 x_1) + \epsilon^{9/2}(\Gamma_3 Y_1^3 + \sigma_3 x_1 Y_1) + \epsilon^6 u_4 + \ldots + E\epsilon^{11/2}[\tilde{u}_0 + \epsilon^{3/2}\tilde{u}_1 + \ldots] + \text{c.c.} + \ldots, \quad (3.1)$$

$$v = \epsilon^6\{\gamma_0 + \epsilon^{3/2}\gamma_1 Y_1 + \epsilon^3 v_2 + \ldots + E\epsilon[\tilde{v}_0 + \ldots] + \text{c.c.} + \ldots\}, \quad (3.2)$$

$$w = \epsilon^6\{\epsilon^{-3}\delta_0 + \epsilon^{-3/2}\delta_{01} Y_1 + (\delta_{02} Y_1^2 + x_1\delta_1) + \epsilon^{3/2} w_0 + \ldots + E\epsilon^{-1/2}[\tilde{w}_0 + \ldots] + \text{c.c.} + \ldots\}, \quad (3.3)$$

$$p = p_{00} + \ldots + \epsilon^6 q_{00} + \epsilon^{15/2} q_{01}\, Y_1 + \epsilon^9 (q_{02}\, Y_1^2 + x_1\, q_{11}) + \epsilon^{21/2} (q_{03}\, Y_1^3 + x_1\, Y_1\, \hat{q}_{03}) + \ldots$$
$$+ E\epsilon^7 [\tilde{p}_0 + \epsilon^{3/2} \tilde{p}_1 + \epsilon^3 (\ln \epsilon)\, \tilde{p}_{2L} + \epsilon^3 \tilde{p}_2 + \epsilon^{9/2} \tilde{p}_3 + \epsilon^6 (\ln \epsilon)\, \tilde{p}_{4L} + \epsilon^6 \tilde{p}_4$$
$$+ \epsilon^{15/2} (\ln \epsilon)\, \hat{p}_{5L} + \epsilon^{15/2} \tilde{p}_5 + \ldots] + \text{c.c.} + \ldots . \tag{3.4}$$

Here the wave terms $\tilde{p}_2, \tilde{p}_4$ grow like $(1, Y_1^2) \ln |Y_1|$ at large $|Y_1|$ to match with the wave forms in §2, whereas $\gamma_0, \gamma_1, \delta_0, \delta_{01}, \delta_{02}, \tilde{p}_{2L}, \tilde{p}_{4L}, \tilde{p}_{5L}$, etc., are constants. In particular $\gamma_0 = V_1(r_0), \delta_0 = W_0(r_0)$. The vital contributions in (3.1)–(3.4) are u_4, v_2, w_0 for the vortex and $\tilde{p}_5$ for the wave part, as is seen below.

3.1. *The vortex components*

The governing equations with (3.1)–(3.4) holding yield the viscous system

$$v_{2Y_1} + r_0^{-1} w_{0\theta} = 0, \tag{3.5}$$

$$(c_0\, \partial_{x_1} + r_0^{-1} \delta_0\, \partial_\theta)\, u_4 + v_2\, \Gamma_1 = u_{4Y_1 Y_1}, \tag{3.6}$$

$$(c_0\, \partial_{x_1} + r_0^{-1} \delta_0\, \partial_\theta)\, w_0 = w_{0Y_1 Y_1}, \tag{3.7}$$

for the mean-flow vortex components apart from polynomial contributions. In comparison with SBB, no extra pressure gradient enters from the centrifugal forces for example but there is a new feature in the δ_0 derivative terms due to the swirl present. These are analogous to the cross-flow contributions of Part 1 and (3.7) above is directly comparable with (3.14*a*) there. The vortex system (3.5)–(3.7), which is subject to the condition that w_0 vanishes at large $|Y_1|$, is forced by a jump condition on $\partial w_0 / \partial Y_1$ at $Y_1 = 0\pm$, due to the nonlinear wave effects within the critical layer, in the form

$$[w_{0Y_1}]_{0-}^{0+} = F(|\tilde{p}_{0\theta}|^2); \tag{3.8}$$

see §4 on the function F. The back-effect of the present vortex contribution is also central to the nonlinear interplay because, in turn, the vortex influences the wave parts below through vortex/wave interaction. In addition the property that v_2 is $O(1)$ at large $|Y_1|$, from integration of (3.5), fixes the power m in §2 to be 9.

3.2. *The wave parts*

From (3.1)–(3.4) the successive wave components satisfy the following balances, which are predominantly inviscid still. First,

$$\mathscr{C}(\tilde{u}_0, \tilde{v}_0, \tilde{w}_0) \equiv \mathrm{i}\alpha_0 \tilde{u}_0 + \tilde{v}_{0Y_1} + r_0^{-1} \tilde{w}_{0\theta} = 0, \tag{3.9}$$

$$\mathscr{X}(\tilde{u}_0, \tilde{v}_0, \tilde{p}_0) \equiv \Gamma_1\, Y_1\, \mathrm{i}\alpha_0 \tilde{u}_0 + \tilde{v}_0\, \Gamma_1 + \mathrm{i}\alpha_0 \tilde{p}_0 = 0, \tag{3.10}$$

$$\tilde{p}_{0Y_1} = 0, \tag{3.11}$$

$$\Theta(\tilde{w}_0, \tilde{p}_0) \equiv \Gamma_1\, Y_1\, \mathrm{i}\alpha_0 \tilde{w}_0 + r_0^{-1} \tilde{p}_{0\theta} = 0. \tag{3.12}$$

Hence the solutions for the r_+ contributions have

$$\tilde{u}_0 = n^2 r_+ / (\alpha_0^2 r_0^2\, \Gamma_1\, Y_1)\, \hat{e}, \quad \tilde{v}_0 = -\mathrm{i} r_+ A / (\alpha_0\, \Gamma_1)\, \hat{e}, \tag{3.13}$$

$$\tilde{w}_0 = -n r_+ / (\alpha_0 r_0\, \Gamma_1\, Y_1)\, \hat{e}, \quad \tilde{p}_0 = r_+(x_1)\, \hat{e}, \tag{3.14}$$

matching with the bulk-flow solutions, and likewise for the r_- contributions.

Secondly, we obtain

$$\mathscr{C}(\tilde{u}_1, \tilde{v}_1, \tilde{w}_1) + r_0^{-1}\tilde{v}_0 - r_0^{-2} Y_1 \tilde{w}_{0\theta} = 0, \tag{3.15}$$

$$\mathscr{X}(\tilde{u}_1, \tilde{v}_1, \tilde{p}_1) + (\Gamma_2 Y_1^2 + c_2 x_1)\, i\alpha_0 \tilde{u}_0 + 2\tilde{v}_0 \Gamma_2 Y_1 + \tilde{\mathscr{L}}(\tilde{u}_0) = 0, \tag{3.16}$$

$$p_{1Y_1} = 0, \tag{3.17}$$

$$\Theta(\tilde{w}_1, \tilde{p}_1) + (\Gamma_2 Y_1^2 + c_2 x_1)\, i\alpha_0 \tilde{w}_0 + \tilde{\mathscr{L}}(\tilde{w}_0) - r_0^{-2} Y_1 \tilde{p}_{0\theta} = 0, \tag{3.18}$$

where the operator $\tilde{\mathscr{L}} \equiv (c, \partial_{x_1} + r_0^{-1}\delta_0\, \partial_\theta - \partial_{Y_1}^2)$. These fix (ii,, $\tilde{v}_1$, $\tilde{w}_1$), with $\tilde{p}_1$ being identically zero.

Thirdly, $(\tilde{u}_2, \tilde{v}_2, \tilde{w}_2, \tilde{p}_2)$ are controlled by

$$\mathscr{C}(\tilde{u}_2, \tilde{v}_2, \tilde{w}_2) + \tilde{u}_{0x_1} + r_0^{-1}\tilde{v}_1 - r_0^{-2} Y_1 \tilde{v}_0 - r_0^{-2} Y_1 \tilde{w}_{1\theta} + r_0^{-3} Y_1^2 \tilde{w}_{0\theta} = 0, \tag{3.19}$$

$$\mathscr{X}(\tilde{u}_2, \tilde{v}_2, \tilde{p}_2) + \Gamma_1 Y_1 \tilde{u}_{0x_1} + \ldots + \tilde{\mathscr{L}}(\tilde{u}_1) + \tilde{p}_{0x_1} = 0, \tag{3.20}$$

$$\tilde{p}_{2Y_1} + \Gamma_1 Y_1\, i\alpha_0 \tilde{v}_0 - 2r_0^{-1}\delta_0 \tilde{w}_0 = 0, \tag{3.21}$$

$$\Theta(\tilde{w}_2, \tilde{p}_2) + \ldots + \tilde{\mathscr{L}}(\tilde{w}_1) + \ldots = 0; \tag{3.22}$$

here and below only newly appearing types of terms are shown explicitly in the main. So far all the terms encountered are in a sense continuations of those in the bulk. We notice especially that the centrifugal term in (3.21) requires $\tilde{p}_2$ to be logarithmic in Y_1, in view of the $\tilde{w}_0$ solution in (3.14), merging both with the bulk response of §2 and the critical-layer response of §4. Again, swirl and other effects are gradually intruding in (3.15)–(3.22), compared with (3.9)–(3.12).

Fourthly, the induced vortex components of §3.1 make their presence felt in the controlling equations

$$\mathscr{C}(\tilde{u}_3, \tilde{v}_3, \tilde{w}_3) + \ldots = 0, \tag{3.23}$$

$$\mathscr{X}(\tilde{u}_3, \tilde{v}_3, \tilde{p}_3) + u_4\, i\alpha_0 \tilde{u}_0 + \tilde{v}_0 u_{4Y_1} + r_0^{-1}\tilde{w}_0 u_{4\theta} + \ldots = 0, \tag{3.24}$$

$$\tilde{p}_{3Y_1} + \Gamma_1 Y_1\, i\alpha_0 \tilde{v}_1 + \ldots = 0, \tag{3.25}$$

$$\Theta(\tilde{w}_3, \tilde{p}_3) + u_4\, i\alpha_0 \tilde{w}_0 + \ldots = 0, \tag{3.26}$$

for $(\tilde{u}_3, \tilde{v}_3, \tilde{w}_3, \tilde{p}_3)$. The new vortex effects as shown explicitly here in the axial and azimuthal momentum balances involve the unknown velocity u_4, which is governed by (3.5)–(3.8), cf. Part 1.

Higher-order terms are still needed however in the radial momentum balance, specifically

$$\tilde{p}_{5Y_1} + u_4\, i\alpha_0 \tilde{v}_0 + \Gamma_1 Y_1\, i\alpha_0 \tilde{v}_3 - 2r_0^{-1}(\delta_0 \tilde{w}_3 + w_0 \tilde{w}_0) + \ldots = 0, \tag{3.27}$$

which shows new vortex (u_4, w,,) and swirl (δ_0) influences. This pressure $\tilde{p}_5$ helps to control the crucial jump across the buffer and critical layer. Combining (3.27) with (3.23)–(3.26) and earlier equations, and retaining only those terms that are affected by the induced vortex flow and swirl, we obtain the equation

$$\tilde{\tilde{p}}_{5Y_1Y_1} - 2Y_1^{-1}\tilde{\tilde{p}}_{5Y_1} = -2\hat{u}_{4Y_1} r_- \Gamma_1^{-1}\left[A + \frac{\delta_0 n}{r_0^2 \alpha_0 \Gamma_1 Y_1^2}\right] + \frac{2nr_-[\hat{w}_{0Y_1}/Y_1 - 3\hat{w}_0/Y_1^2]}{r_0^2 \alpha_0 \Gamma_1}$$
$$+ \frac{2\hat{u}_4 r_-[A + 2n^2/r_1^2 \Gamma_1 Y_1 + 4\delta_0 n/(r_0^2 \alpha_0 \Gamma_1 Y_1^2)]}{} \tag{3.28}$$

for the corresponding $r_+ \hat{e}$ part $\tilde{\tilde{p}}_5$ of $\tilde{p}_5$. Here $\hat{u}_4$, $\hat{w}_0$ are the $\hat{e}^2$ (forced) parts of u_4, w_0 (see (3.8)), explaining the presence of the r_- contributions in (3.28). Our main concern now is with the $O(Y_1)$ terms at large $|Y_1|$, since only these affect the jump $(\tilde{J})$ in the

$O(Y_1^3)$ part of $\tilde{p}_5$ across the entire buffer required to match the $O(s^3)$ jump described in §2.1. From integration of (3.28) across the buffer, and then equating $\tilde{J}$ with the jump described after (2.26), the balance

$$r_-\left(\frac{2n^2}{r_0^2}-\Lambda\right)\frac{inT_0}{c_0}+(D^+-D^-)=\frac{\Gamma_1^2}{r_0}\{x_1 r_+(G_a^+-G_a^-)+ic_0 r'_+(G_b^+-G_b^-)+\sigma r_+(G_c^+-G_c^-)\} \tag{3.29}$$

is produced. Here (D^+-D^-) denotes the jump across the critical layer (for $Y_1\to 0\pm$) as described in the next section, while

$$T_0\equiv -2ic_0\Gamma_1^{-1}n^{-1}\int_0^\infty Y_1^{-1}\hat{u}_{4Y_1Y_1}\,dY_1 \tag{3.30}$$

given that $\hat{u}_{4Y_1Y_1}$ is zero at $Y_1=0\pm$. The extra swirl effects in (3.28) for instance are found to add nothing as far as the jump above is concerned, thus leaving (3.29) essentially the same as SBB's equation (5.1), apart from the additional σ term on the right in (3.29).

4. The critical layer

In the critical layer the buffer coordinate Y_1 essentially becomes $O(\epsilon^{1/2})$, leaving $r=\epsilon^6(r_0+\epsilon^2 Y)$ with Y of order unity, and so

$$u=c_0+\epsilon^2\Gamma_1 Y+\epsilon^3 c_2 x_1+\epsilon^4\Gamma_2 Y^2+\epsilon^5\bar{u}_0+\epsilon^6\bar{u}_1+\epsilon^7\bar{u}_2+\ldots, \tag{4.1}$$

$$v=\epsilon^6\{\gamma_0+\epsilon\bar{v}_2+\epsilon^2\bar{v}_3+\ldots\}, \tag{4.2}$$

$$w=\epsilon^6\{\epsilon^{-3}\delta_0+\epsilon^{-1}\bar{w}_0+\bar{w}_1+\ldots\}, \tag{4.3}$$

$$p=p_0+\epsilon^6 q_{00}+\epsilon^7\bar{p}_2+\epsilon^8\bar{p}_3+\epsilon^9\bar{p}_4+\epsilon^{10}\bar{p}_5+\ldots, \tag{4.4}$$

from §3. Additional terms, e.g. in $\ln\epsilon$, should be included but they have only a passive effect here as in SBB. Matching requires among other things that, at large $|Y|$, $\bar{u}_{0N}\sim\sigma_3 x_1 Y$, $\bar{u}_{0E}\propto Y^{-1}$, $\bar{u}_{1N}\sim\Gamma_3 Y^3+u_4$ (at $Y_1=0\pm$), $\bar{v}_2$ is $O(1)$, $\bar{v}_{3N}\sim\gamma_1 Y$, $\bar{w}_{0N}\sim\delta_{01}Y$, $\bar{w}_{0E}\propto Y^{-1}$, $\bar{w}_{1N}\sim\delta_1 x_1$, $\bar{w}_{2N}\sim\delta_{02}Y^2$, $\bar{w}_{5/2N}\sim w_0$ (at $Y_1=0\pm$), $\bar{w}_{3N}\sim Y_1\partial w_0/\partial Y_1$ (at $Y_1=0\pm$), where the subscripts N,E denote the mean and fluctuating parts of the velocity and pressure, respectively. The constant $\sigma_3=6c_0^{-1}\Gamma_3+(2\Gamma_2-r_0^{-1}\Gamma_1)(r_0^{-1}-\gamma_0)$, and the values at $Y_1=0\pm$ are due to the induced vortex (§3.1) in the buffer. The resulting balances given below confirm that the wave part now responds in a viscous–inviscid fashion whereas the vortex part is mostly viscous. We need to proceed through several orders in the governing equations.

4.1. *Continuity balances*

From substitution into (1.1), and with $\bar{\mathscr{C}}(u,w)$ referring to $\partial u/\partial X+r_0^{-1}\partial w/\partial\theta$, the successive continuity balances are

$$\bar{\mathscr{C}}(\bar{u}_0,\bar{w}_0)=0, \tag{4.5}$$

$$\bar{\mathscr{C}}(\bar{u}_1,\bar{w}_1)+c_2+\bar{v}_{3Y}+r_0^{-1}\gamma_0=0, \tag{4.6}$$

$$\bar{\mathscr{C}}(\bar{u}_2,\bar{w}_2)+\bar{v}_{4Y}+r_0^{-1}\bar{v}_2-r_0^{-2}Y\bar{w}_{0\theta}=0, \tag{4.7}$$

$$\bar{\mathscr{C}}(\bar{u}_3,\bar{w}_3)+\bar{u}_{0x_1}+\bar{v}_{5Y}+r_0^{-1}\bar{v}_3-r_0^{-2}Y(\gamma_0+\bar{w}_{1\theta})=0, \tag{4.8}$$

$$\bar{\mathscr{C}}(\bar{u}_4,\bar{w}_4)+\bar{u}_{1x_1}+\bar{v}_{6Y}+r_0^{-1}\bar{v}_4-r_0^{-2}Y(\bar{v}_2+\bar{w}_{2\theta})+r_0^{-3}Y^2\bar{w}_{0\theta}=0, \tag{4.9}$$

$$\bar{\mathscr{C}}(\bar{u}_5,\bar{w}_5)+\bar{u}_{2x_1}+\bar{v}_{7Y}+r_0^{-1}\bar{v}_5-r_0^{-2}Y(\bar{v}_3+\bar{w}_{3\theta})+r_0^{-3}Y^2(\gamma_0+\bar{w}_{1\theta})=0, \tag{4.10}$$

from orders ϵ^{-1} to ϵ^4 in turn. Mean-flow, non-parallel and rotation influences are observed to enter play gradually. The main wave is controlled by (4.5) but we need to proceed to the wave part in (4.10) also, while mean vortex effects first appear in (4.8).

4.2. x-Momentum balances

Here (1.2) yields the governing equations, from the orders 1 to ϵ^6 respectively,

$$c_0 c_2 + \gamma_0 \Gamma_1 = 2\Gamma_2 + r_0^{-1}\Gamma_1, \tag{4.11}$$

$$\mathscr{X}_0 = 0, \tag{4.12}$$

$$\mathscr{X}_1 + \Gamma_1 Y c_2 + \mathscr{F}_1 \bar{u}_0 + 2\gamma_0 \Gamma_2 \mathrm{Y} = -r_0^{-2} Y \Gamma_1 + 2r_0^{-1}\Gamma_2 Y, \tag{4.13}$$

$$\bar{\mathscr{X}}_2 + \mathscr{F}_1 \bar{u}_1 + c_2^2 x_1 + \Gamma_2 Y^2 \bar{u}_{0EX} + \gamma_0 \bar{u}_{0Y} + 2\bar{v}_2 \Gamma_2 \mathrm{Y} = r_0^{-1}\bar{u}_{0Y}, \tag{4.14}$$

$$\begin{aligned}\mathscr{X}_3 + \Gamma_1 Y \bar{u}_{0x_1} + \mathscr{F}_1 \bar{u}_2 + \Gamma_2 Y^2(\bar{u}_{1EX} + c_2) + \bar{u}_0 \bar{u}_{0EX} + \gamma_0 \bar{u}_{1Y} + 2\bar{v}_3 \Gamma_2 Y + \bar{v}_2 \bar{u}_{0Y} \\ + r_0^{-1}\bar{w}_0 \bar{u}_{0\theta} - r_0^{-2} Y \delta_0 \bar{u}_{0\theta} = -\bar{p}_{2x_1} + r_0^{-1}\bar{u}_{1Y} + r_0^{-3} Y^2 \Gamma_1 - 2r_0^{-2}\Gamma_2 Y^2,\end{aligned} \tag{4.15}$$

$$\begin{aligned}\bar{\mathscr{X}}_4 + \Gamma_1 Y \bar{u}_{1x_1} + \mathscr{F}_1 \bar{u}_3 + c_2 x_1 \bar{u}_{0x_1} + \Gamma_2 Y^2 \bar{u}_{2EX} + \bar{u}_0(\bar{u}_{1EX} + c_2) \\ + \bar{u}_1 \bar{u}_{0EX} + \gamma_0 \bar{u}_{2Y} + \bar{v}_2 \bar{u}_{1Y} + \bar{v}_3 \bar{u}_{0Y} + 2\bar{v}_4 \Gamma_2 Y + r_0^{-1}(\bar{w}_0 \bar{u}_{1\theta} + \bar{w}_1 \bar{u}_{0\theta}) \\ - r_0^{-2} Y \delta_0 \bar{u}_{1\theta} = -\bar{p}_{3x_1} + r_0^{-1}\bar{u}_{2Y} - r_0^{-2} Y \bar{u}_{0Y} + r_0^{-2}\bar{u}_{0\theta\theta} + \bar{u}_{0EXX},\end{aligned} \tag{4.16}$$

$$\begin{aligned}\bar{\mathscr{X}}_5 + \Gamma_1 Y \bar{u}_{2x_1} + \mathscr{F}_1 \bar{u}_4 + c_2 x_1 \bar{u}_{1x_1} + \Gamma_2 Y^2(\bar{u}_{3EX} + \bar{u}_{0x_1}) \\ + \bar{u}_0 \bar{u}_{2EX} + \bar{u}_1(\bar{u}_{1EX} + c_2) + \bar{u}_2 \bar{u}_{0EX} + \gamma_0 \bar{u}_{3Y} + \bar{v}_2 \bar{u}_{2Y} + \bar{v}_3 \bar{u}_{1Y} + \bar{v}_4 \bar{u}_{0Y} \\ + 2\bar{v}_5 \Gamma_2 Y + r_0^{-1}(\bar{w}_0 \bar{u}_{2\theta} + \bar{w}_1 \bar{u}_{1\theta} + \bar{w}_2 \bar{u}_{0\theta}) - r_0^{-2} Y(\delta_0 \bar{u}_{2\theta} + \bar{w}_0 \bar{u}_{0\theta}) + r_0^{-3} Y^2 \delta_0 \bar{u}_{0\theta} \\ = -\bar{p}_{4x_1} + r_0^{-1}\bar{u}_{3Y} - r_0^{-2} Y \bar{u}_{1Y} + (2r_0^{-3}\Gamma_2 - r_0^{-4}\Gamma_1) Y^3 + r_0^{-2}\bar{u}_{1\theta\theta} + \bar{u}_{1EXX},\end{aligned} \tag{4.17}$$

with $\bar{\mathscr{X}}_k$ for $k \geqslant 0$ denoting $\Gamma_1(Y \partial \bar{u}_{kE}/\partial X + \bar{v}_{k+2}) + \partial \bar{p}_{k+2E}/\partial X - \partial^2 \bar{u}_k/\partial Y^2$. The operator $\mathscr{F}_1$ is $(c_2 x_1 \partial_X + c_0 \partial_{x_1} + r_0^{-1}\delta_0$ a,). The mean terms in (4.11) agree with the mean balance obtained in § 2.1. The subsequent balances again show the influences of non-parallel, mean, rotation and swirl forces entering, with the main wave in (4.12), the final wave part to be examined in (4.17), the input mean flow present in (4.1 1), (4.13) ff., and the induced vortex in (4.15).

The terms $\bar{v}_5 \Gamma_1, \bar{p}_{5X}$ in (4.15) provoke an extra logarithmic response as anticipated earlier but this produces little impact on the major vortex/wave interaction eventually, as we shall see.

4.3. r-Momentum balances

From (1.3) we have the successive balances, at orders ϵ^{-1} through to ϵ^4,

$$(0, -r_0^{-1}\delta_0^2, 0) = -(\bar{p}_{2Y}, \bar{p}_{3Y}, \bar{p}_{4Y}), \tag{4.18}$$

$$-2r_0^{-1}\delta_0 \bar{w}_0 + r_0^{-2} Y \delta_0^2 = -\bar{p}_{5Y}, \tag{4.19}$$

$$\Gamma_1 Y \bar{v}_{2EX} - 2r_0^{-1}\delta_0 \bar{w}_1 = -\bar{p}_{6Y} + \bar{v}_{2YY}, \tag{4.20}$$

$$\Gamma_1 Y \bar{v}_{3EX} + \mathscr{F}_1 \bar{v}_2 - r_0^{-1}(2\delta_0 \bar{w}_2 + \bar{w}_0^2) + 2r_0^{-2} Y \delta_0 \bar{w}_0 - r_0^{-3} Y^2 \delta_0^2 = -\bar{p}_{7Y} + \bar{v}_{3YY}. \tag{4.2 1}$$

The main wave result is simply that $\bar{p}_2$ is independent of Y, and likewise for $\bar{p}_4$, while the final wave part needed is in (4.2 1). The first non-trivial Y-dependence arises in (4.19) from the swirl effect δ_0, which also promotes additional Y-dependence at higher orders. The balance in (4.19) produces an interesting logarithmic feature which is addressed subsequently.

4.4. *θ-Momentum balances*

The balances resulting from (1.4) at orders ϵ through to ϵ^6 are, with $\bar{\Theta}_k$ denoting $\Gamma_1 Y\partial\bar{w}_{kE}/\partial X + r_0^{-1}\partial\bar{p}_{k+2}/\partial\theta - \partial^2\bar{w}_k/\partial Y^2$ $(k \geqslant 0)$,

$$\bar{\Theta}_0 = 0, \tag{4.22}$$

$$\bar{\Theta}_1 + \mathscr{F}_1\bar{w}_0 = 0, \tag{4.23}$$

$$\bar{\Theta}_2 + \mathscr{F}_1\bar{w}_1 + \Gamma_2 Y^2\bar{w}_{0EX} + \gamma_0\bar{w}_{0Y} + r_0^{-1}\gamma_0\delta_0 = r_0^{-2}Y\bar{p}_{2\theta} + r_0^{-1}\bar{w}_{0Y} - r_0^{-2}\delta_0, \tag{4.24}$$

$$\bar{\Theta}_3 + \Gamma_1 Y\bar{w}_{0x_1} + \mathscr{F}_1\bar{w}_2 + \Gamma_2 Y^2\bar{w}_{1EX} + \bar{u}_0\bar{w}_{0EX} + \gamma_0\bar{w}_{1Y} + \bar{v}_2\bar{w}_{0Y} + r_0^{-1}(\bar{w}_0\bar{w}_{0\theta} + \delta_0\bar{v}_2) - r_0^{-2}Y\delta_0\bar{w}_{0\theta} = r_0^{-2}Y\bar{p}_{3\theta} + r_0^{-1}\bar{w}_{1Y}, \tag{4.25}$$

$$\begin{aligned}\bar{\Theta}_4 &+ \Gamma_1 Y\bar{w}_{1x_1} + \mathscr{F}_1\bar{w}_3 + c_2 x_1\bar{w}_{0x_1} + \Gamma_2 Y^2\bar{w}_{2EX} + (\bar{u}_0\bar{w}_{1EX} + \bar{u}_1\bar{w}_{0EX}) \\ &+ \gamma_0\bar{w}_{2Y} + (\bar{v}_2\bar{w}_{1Y} + \bar{v}_3\bar{w}_{0Y}) + r_0^{-1}((\bar{w}_0\bar{w}_1)_\theta + \delta_0\bar{v}_3 + \gamma_0\bar{w}_0) - r_0^{-2}Y(\delta_0\bar{w}_{1\theta} + \gamma_0\delta_0) \\ &= r_0^{-2}Y\bar{p}_{4\theta} - r_0^{-3}Y^2\bar{p}_{2\theta} + r_0^{-1}\bar{w}_{2Y} - r_0^{-2}(Y\bar{w}_{0Y} - \bar{w}_{0\theta\theta} + \bar{w}_0) + 2r_0^{-3}Y\delta_0 + \bar{w}_{0EXX},\end{aligned} \tag{4.26}$$

$$\begin{aligned}\bar{\Theta}_5 &+ \Gamma_1 Y\bar{w}_{2x_1} + \mathscr{F}_1\bar{w}_4 + c_2 x_1\bar{w}_{1x_1} + \Gamma_2 Y^2(\bar{w}_{3EX} + \bar{w}_{0x_1}) + (\bar{u}_0\bar{w}_{2EX} + \bar{u}_1\bar{w}_{1EX} \\ &+ \bar{u}_2\bar{w}_{0EX}) + \gamma_0\bar{w}_{3Y} + (\bar{v}_2\bar{w}_{2Y} + \bar{v}_3\bar{w}_{1Y} + \bar{v}_4\bar{w}_{0Y}) + r_0^{-1}((\bar{w}_0\bar{w}_2)_\theta \\ &+ \bar{w}_1\bar{w}_{1\theta} + \delta_0\bar{v}_4 + \gamma_0\bar{w}_1 + \bar{v}_2\bar{w}_0) - r_0^{-2}Y(\delta_0\bar{w}_{2\theta} + \bar{w}_0\bar{w}_{0\theta} + \bar{v}_2\delta_0) + r_0^{-3}Y^2\delta_0\bar{w}_{0\theta} \\ &= r_0^{-2}Y\bar{p}_{5\theta} - r_0^{-3}Y^2\bar{p}_{3\theta} + r_0^{-1}\bar{w}_{3Y} - r_0^{-2}(Y\bar{w}_{1Y} - \bar{w}_{1\theta\theta} + \bar{w}_1) + \bar{w}_{1EXX}.\end{aligned} \tag{4.27}$$

The dominant wave equation is therefore (4.22), the dominant induced-vortex equation is contained in (4.25) and the final wave equation of concern is (4.27).

4.5. *Solutions*

To solve (4.5)–(4.27) for $\bar{u}_{0E}, \bar{w}_{0E}$ and so on, we combine the x- and θ-momentum balances, along with those of continuity, to find the skewed shears $Q \equiv \partial\bar{u}/\partial X + r_0^{-1}\partial\bar{w}/\partial\theta$. The fluctuating parts are split as $\bar{u}_{0E} = E\bar{u}_{0E} + \text{c.c.}$, etc., allowing $\partial X, \partial_\theta$ to be replaced by $\mathrm{i}\alpha_0$, $\mathrm{i}n$ in most places, e.g. in $\mathscr{F}_1$.

First, (4.5), (4.12), (4.18), (4.22) yield the dominant wave and mean solutions as

$$Q_{0E} = 0, \quad (\bar{\bar{u}}_{0E}, \bar{\bar{w}}_{0E}) = \left(-\frac{\mathrm{i}n^2}{\alpha_0 r_0^2}, \frac{\mathrm{i}n}{r_0}\right)\bar{\bar{p}}_{2E}\mathscr{L}, \tag{4.28}$$

$$\bar{\bar{v}}_{2E} = -\mathrm{i}\alpha_0^{-1}\Gamma_1^{-1}A\bar{\bar{p}}_{2E}, \quad \bar{u}_{0N} = \sigma_3 x_1 Y, \quad \bar{w}_{0N} = \delta_{01}Y, \quad \bar{v}_{2N} = \bar{p}_{2N} = 0, \tag{4.29}$$

where the function $\mathscr{L}(Y)$ satisfies $\mathscr{L}'' - BY\mathscr{L} = 1$ with $\mathscr{L} \sim -B^{-1}Y^{-1}$ at large $|Y|$ and can be expressed in integral form as in SBB. The constant $B = \Gamma_1\mathrm{i}\alpha_0$ and $\bar{\bar{p}}_{2E} = \tilde{p}_0$ as given in (3.14).

Secondly, a similar procedure is found to give the solutions

$$Q_{1E} = A_{1E}, \quad \bar{\bar{u}}_{1E} = B_1\mathscr{L}' + C_1, \quad \bar{\bar{w}}_{1E} = \mathscr{F}_1\bar{\bar{p}}_{2E}\mathrm{i}n\mathscr{L}'/(Br_0), \tag{4.30}$$

$$\bar{\bar{v}}_{3E} = \bar{\bar{p}}_{3E} = 0, \quad \bar{u}_{1N} = \Gamma_3 Y^3 + u_4(x_1, 0, \theta), \quad \bar{w}_{1N} = \delta_1 x_1, \tag{4.31}$$

with

$$\mathrm{i}\alpha_0 C_1 = A_{1E}, \quad B_1 = -\mathscr{F}_1\bar{\bar{p}}_{2E}n^2/(\Gamma_1\alpha_0^2 r_0^2), \tag{4.32}$$

from (4.6), (4.13), (4.18), (4.23). Here matching with the buffer determines the function $A_{1E}(x_1, \theta)$ (and hence C_1) to be zero. Third, and after matching again,

$$Q_{2E} = A_{2E} + q_{22}\mathscr{L}'', \quad q_{22} = \bar{\bar{p}}_{2E}/(3Br_0^3), \quad \bar{\bar{p}}_{4E} = 0, \tag{4.33}$$

$$\bar{\bar{w}}_{2E} = \sigma_{2E} + \sigma_{22}\mathscr{L}'' + \sigma_{25}\mathscr{L}^v, \quad \bar{\bar{v}}_{4E} = t_{4E}Y + 2q_{22}\mathscr{L}', \tag{4.34}$$

$$\bar{u}_{2N} = \sigma_4 x_1 Y^2, \quad \bar{w}_{2N} = \delta_{02}Y^2, \quad \bar{v}_{2N} = 0. \tag{4.35}$$

Here the constant σ_4 can be related to the constant Γ_4 in (2.9), and $\sigma_{2E}, \sigma_{22}, \sigma_{25}, t_{4E}$ are functions of x_1 and θ and are given in the Appendix. The function $A_{2E}(x_1, \theta)$ may be determined by matching with the buffer solution and is found to involve the constant q_3 in (2.21). Fourthly

$$Q_{3E} = q_{30}\mathscr{L} + q_{33}\mathscr{L}''', \quad \bar{\bar{w}}_{3E} = \sigma_{30}\mathscr{L} + \sigma_{33}\mathscr{L}''' + \sigma_{36}\mathscr{L}^{\mathrm{vi}} - 2\delta_0 r_0^{-3} n^2 \bar{\bar{p}}_{2E}\mathscr{M}, \tag{4.36}$$

$$\bar{\bar{p}}_{5E} = 2\delta_0 r_0^{-2} \mathrm{i}n \bar{\bar{p}}_{2E} \int \mathscr{L}\,\mathrm{d}Y, \quad \bar{\bar{v}}_{5E} = (\Lambda/B)\bar{\bar{p}}_{5E} + t_{5E} + t_{52}\mathscr{L}'' \tag{4.37}$$

with the function $\mathscr{M}$ and the more significant coefficients being shown in the Appendix. Fifthly,

$$Q_{4E} = A_{4E} + B_{4E}\,Y + q_{41}\mathscr{L}' + q_{44}\mathscr{L}^{\mathrm{iv}} + q_{47}\mathscr{L}^{\mathrm{vii}}; \tag{4.38}$$

again see the Appendix.

Sixthly, and lastly as regards the wave parts, we find the equation

$$Q_{5EYYY} - BYQ_{5EY} = \mathrm{RHS}_5 \tag{4.39}$$

for the effective vorticity Q_{5EY}. The detailed expression RHS_5, which is long and complicated, is available from the authors. The only terms within it that matter with regard to matching at large $|Y|$ and fixing the crucial jump condition are independent of Y. The total of these terms, χ say, is also given in the Appendix; the remainder of RHS_5 is a sum of terms each proportional to $\mathscr{L}^{(r)}$ for some $r \geqslant 0$. Since $\mathscr{L}^{(r)}$ in RHS_5 leads to a multiple of $\mathscr{L}^{(r)}$ in Q_{5E} all of which tend to zero as $|Y| \to \infty$, the only contribution to the logarithmic behaviour of Q_{5E} at large $|Y|$ is derived from χ to be

$$-B^{-1}\chi \int \mathscr{L}\,\mathrm{d}Y. \tag{4.40}$$

This form implies that the usual quasi-linear phase shift holds, namely

$$\ln|Y| \to \ln Y + \mathrm{i}(\operatorname{sgn}\Gamma_1)\pi \tag{4.41}$$

as Y changes from large and negative to large and positive, despite all the extra complications in (4.33)–(4.39). The above therefore conforms with the result for $(D^+ - D^-)$ essentially given in Part 1 and SBB.

Concerning next the induced vortex motion, the balance involved is in (4.25), namely

$$[-\mathrm{i}\alpha_0 \bar{\bar{u}}_{0E}\bar{\bar{w}}^*_{0E} + \bar{\bar{v}}_{2E}\bar{\bar{w}}^*_{0EY} + r_0^{-1}\bar{\bar{w}}_{0E}\bar{\bar{w}}^*_{0E\theta}] + \mathrm{c.c.} = \bar{w}_{3NYY}, \tag{4.42}$$

from the vortex terms independent of E. Upon insertion of the wave expressions (4.28), (4.29) in the left-hand side of (4.42), and then integration in Y, the jump $[\bar{w}_{3NY}]_{-\infty}^{\infty}$ is obtained. The result is that anticipated in the buffer-vortex problem of §3.1, with the forcing function F in (3.8) being a real multiple of the forcing function in Part 1.

The final point here is on the appearance of extra logarithmic factors relatively early in the procedure and, later, logarithm squared terms, stemming from the swirl δ_0. These are of interest although they have negligible effects on the major results at the ends of the previous two paragraphs, owing to cancellations. Thus $\bar{\bar{w}}_{3E}$ in (4.36) and hence $\bar{\bar{u}}_{3E}$ both contain $O(Y^{-1}\ln|Y|)$ terms at large $|Y|$ (due to the function $\mathscr{M}$) even though they combine to leave Q_{3E} non-logarithmic, in (4.36). Along with that, $\bar{\bar{p}}_{5E} \propto \delta_0 \ln|Y|$ at large $|Y|$ from (4.37), yielding a finite jump effect in $\bar{\bar{p}}_{5E}$ there (cf. (4.41) and hence in $\tilde{p}_2$ across $Y_1 = 0\pm$ in the buffer of §3.2. The logarithm in $\bar{\bar{p}}_{5E}$ is consistent also with the logarithmic behaviour of $\tilde{p}_2$ locally and thence with the $O(\delta_0 \ln|\bar{r} - r_0|)$ part of $p^{(1)}$ in the core of §2.2. The corresponding jump effect in $p^{(1)}$ forces multiples of $u^{(0)}, v^{(0)}, w^{(0)}, p^{(0)}$ to be added to $u^{(1)}, v^{(1)}, w^{(1)}, p^{(1)}$ (as noted earlier in §2) which match exactly with the jumps induced in $\bar{\bar{u}}_{3E}, \bar{\bar{v}}_{5E}$ for example. Moreover the extra logarithms in $\bar{\bar{w}}_{3E}, \bar{\bar{u}}_{3E}, \bar{\bar{p}}_{5E}$, $\bar{\bar{v}}_{5E}$ add a number of terms to the central equation (4.39) for Q_{5E} which individually

yield $(\ln|Y|)^2$ growths in Q_{5E}; however the cumulative effect is found to cancel out, leaving only $\ln|Y|$ growth as in (4.40) and hence the result (4.41).

5. Solution properties for the Squire jet and related profiles

As a consequence of the swirl contribution $G_c^+ - G_c^-$ described near the end of §2, the governing equations take the form

$$Ct'_{\pm} + At_{\mp} \int_{x_0}^{x_1} t_{\mp}^* t_{\pm} \, ds + (Bx_1 \pm F) t_{\pm} = 0. \qquad (5.1\,a, b)$$

Here the notation is adopted from §3 of Part 1 with $t_{\pm}(x_1)$ being the unknown scaled amplitudes and primes denoting derivatives with respect to x_1. The constants A, B, C, F are such that A is real and the others complex. Equations (5.1) may be compared with (3.16) of Part 1; the latter have $\pm F$ replaced by $F_{\pm}$ where $F_{\pm}$ contain a common wall-layer contribution not present here, and the subsequent analysis there was restricted to a cross-flow for which only the real parts of $F_{\pm}$ differed in the two equations.

The coefficients in (5.1) have been calculated for the Squire jet profiles $U_0(\bar{r}) = 1/(1+\bar{r}^2)^2$ with $n = 1$; see figure 2 and caption. As a representative swirl profile the Batchelor vortex $W_0(\bar{r}) = (1-e^{-\bar{r}^2})/\bar{r}$ was chosen. If a rescaling of $t_{\pm}$ and x_1 in (5.1) is adopted so that $A = 1 = |B| = |C|$ the coefficients are found to be

$$B = -0.219 + 0.976\mathrm{i}, \quad C = -0.992 + 0.123\mathrm{i}, \quad F = 5.22 \times 10^{-2} + 0.863\mathrm{i}. \qquad (5.2)$$

Numerical solutions of (5.1) have been obtained using central differences and Newton iteration. Figures 3 and 4 show that, for the choice of coefficients in (5.2), the ultimate behaviour depends on the form of the initial conditions. In figure 3(*a*) for which $x_0 = 0$ and $t_+ = 0.1, t_- = 0.2$ at $x_1 = 0$, the moduli of the amplitudes decay exponentially to zero at large positive x_1. However in figure 3(*b*), for which $t_+ = 1.0, t_- = 0.75$ at $x_1 = 0$, and the inverse amplitudes are plotted, the initial values are sufficiently large for the nonlinear term in (5.1) to come into effect and a terminating singularity is encountered at a finite value of x_1. This is similar to the singularity in SBB and has $t_+ \approx t_- \approx a_0/(x_s - x_1)^{1+\mathrm{i}\sigma}$ as $x_1 \to x_s - 0$, with the real number σ and complex a_0 related by $C(1+\mathrm{i}\sigma) + A|a_0|^2 = 0$.

It is instructive to investigate other possible downstream behaviours of solutions to (5.1) when the signs of various coefficients in (5.2) are changed. A change of sign of all of B, C, F and the same initial conditions as in figure 3(*b*) results now (see figure 4) in a solution eventually dominated by Gaussian decay similar to that of figure 3(*a*). A change of sign of the non-parallel term B only, together with the initial conditions of figure 3(*a*), leads to a terminating singularity; this case is shown in figure 5.

Possibly the most interesting situation occurs if the signs of both C and F in (5.2) are changed. This choice results in the bounded or quasi-bounded response, as examined in SBB and Part 1, for a wide range of input conditions upstream, confirming previous assumptions about the starting conditions for such solutions. Here 'quasi-bounded' refers to solutions which persist indefinitely far downstream on the present scales with continued or continual nonlinear interplay occurring. An example, with the same conditions as for figure 3(*a*), is shown in figure 6.

The above discussion, for variations in the constants derived from a particular choice of the two profiles, axial and swirl, illustrates the possible downstream behaviour of perturbations initiated at the position $x_1 = 0$. Figure 3(*a*, *b*) demonstrates that whether the termination is in Gaussian decay or an algebraic singularity can

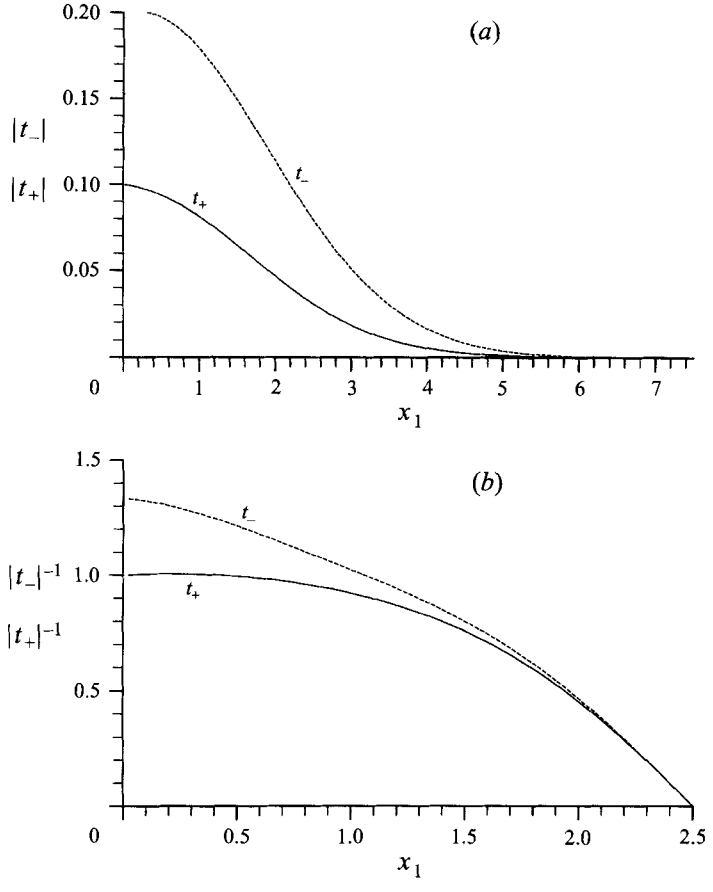

FIGURE 3. (*a*) The moduli of the amplitudes with constants as in (5.2). Here $t_+(0) = 0.1, t_-(0) = 0.2$. (*b*) The inverse of the moduli of the amplitudes. Here $t_+(0) = 1.0, t_-(0) = 0.75$ but otherwise as in (*a*).

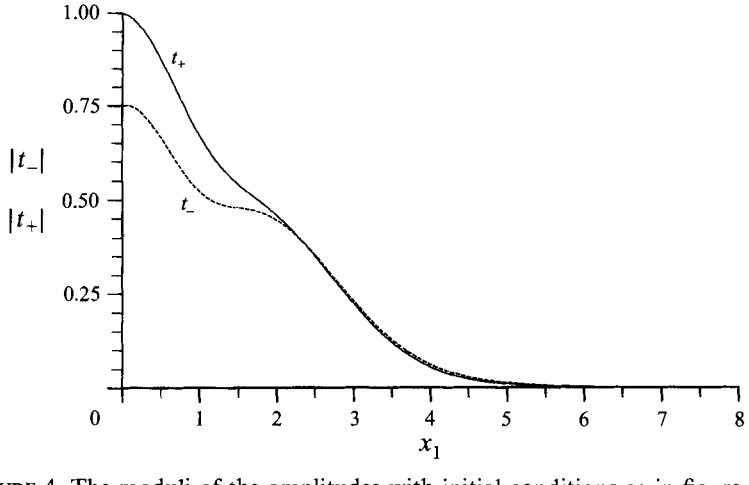

FIGURE 4. The moduli of the amplitudes with initial conditions as in figure 3(*b*) but a change of sign of B, C and F.

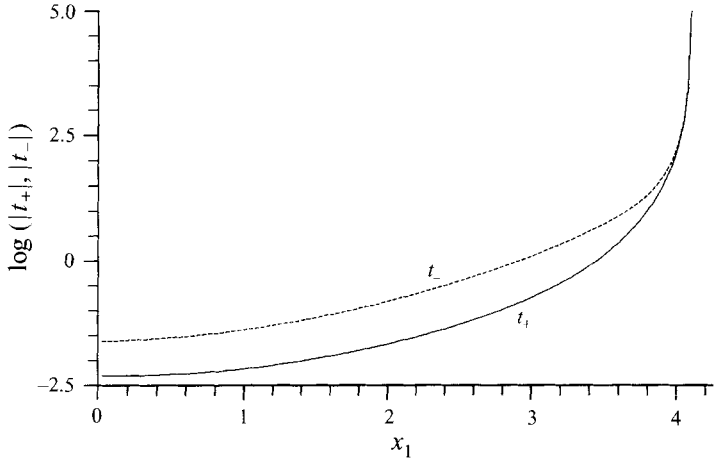

FIGURE 5. The logarithm of the moduli of the amplitudes with conditions as in figure 3(*a*) but with a change of sign of the non-parallel term *B*.

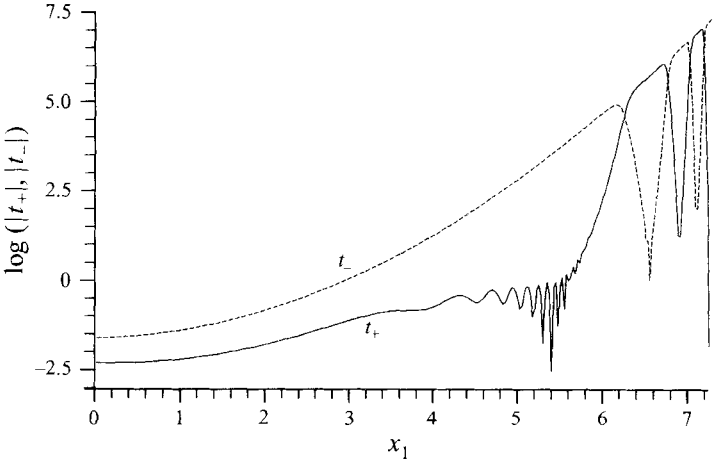

FIGURE 6. As in figure 5 but with a change of sign of *C* and *F* rather than of *B*.

depend on the initial conditions. Quasi-boundedness, as in figure 6, seems to be a consequence of the choice of coefficients, in particular their relative signs, and to occur regardless of the input data. Increase in $|F|$ corresponds to stronger swirl and for the quasi-bounded situation forces transition to enter sooner, in the spatial sense, if transition is interpreted here as nonlinear interactive behaviour; increase in the input amplitudes has a similar result. A final comment concerns the effect of the non-parallel term Bx_1 in (5.1): it controls the Gaussian decay in figures 3(*a*) and 4, and determines the envelope in the quasi-bounded solution of figure 6.

6. Further comments

The study of §§2–5 implies that the resultant nonlinear governing equations for the vortex/wave interaction in the present context of slowly swirling near-axisymmetric jet flows or longitudinal vortices are in essence the same as those in Part 1 where relatively slow cross-flow in a near-planar boundary layer is addresed. The additional effect of

the swirl is felt mainly by the corrections $Ep^{(1)}$ etc. in (2.1)–(2.4) to which have to be added multiples of $Ep^{(0)}$, discontinuous at the critical layer, to accommodate the stronger singularity in (2.25). Despite these complications, which introduce extra logarithmic terms into the details of the analysis and would be significant in any quantitative comparisons of the wave profiles predicted here and measured profiles, the form of the resulting equation is the same. To make the identification it is necessary, as explained in §5, to set the wall-layer effect of Part 1 to zero and to consider a general cross-flow profile. The reason for the similarity of the final equations in the two situations is that the primary ingredients of the vortex/wave interaction, namely wave-squared forcing of the induced vortex flow as in §3.1 and in turn the mean vortex influence on the wave response as in §3.2, are unaltered between Parts 1 and 2. In §5 we have presented solutions of the full integro-differential equations, a task not undertaken in Part 1 which was mainly devoted to an analytical study of the quasi-bounded solutions.

Some other points of relevance here are equivalent to those in Part 1, including the influence of increasing cross-flow (and here swirl) and the many solution paths available depending on the coefficients in the amplitude equations. The present study shows more of the detailed appearance of the swirl effects in the buffer and critical layers. It is likely that a slight increase in the typical input swirl velocity, above its present $O(\epsilon^3)$ level, and/or change of the amplitudes and scales, will substantially alter the overall flow structure in an interesting way, taking us more towards the realistic situation of $O(1)$ swirl velocities. This may provide a basis for alternative descriptions of incipient and eventually catastrophic vortex breakdown, both phenomena of considerable interest and importance.

Thanks are due to Professor M. R. Foster and Dr D. A. R. Davis for discussions, and to the Army Research Office (contract no. DAAL03-92-G-0040) through Dr T. Doligalski for support for F.T.S.

Appendix

The function $\mathscr{M}$ is defined by

$$\mathscr{M}''-BY\mathscr{M}=\int\mathscr{L} \tag{A 1}$$

and the coefficients in (4.34)–(4.38) that are required to calculate χ in (4.40) are given by

$$\sigma_{2E}=(3-2n^2r_0^{-2}\Lambda^{-1})\,\mathrm{i}n\bar{\bar{p}}_{2E}/(2Br_0^2), \tag{A 2}$$

$$\sigma_{22}=(B^{-1}\mathscr{F}_1^2+\gamma_0-2r_0^{-1}+2n^2r_0^{-3}\Lambda^{-1})\,\mathrm{i}n\bar{\bar{p}}_{2E}/(2Br_0), \tag{A 3}$$

$$\sigma_{25}=(1-2r_0^{-2}n^2\Lambda^{-1})\,\mathrm{i}n\bar{\bar{p}}_{2E}/(10B^2r_0^2), \tag{A 4}$$

$$t_{4E}=-A_{2E}-\alpha_0^2\bar{\bar{p}}_{2E}/(Br_0), \tag{A 5}$$

$$q_{30}=[n^2(r_0^{-1}\mathscr{F}_1-\Gamma_1\partial_{x1})-2\delta_0\,\mathrm{i}n\Lambda]\bar{\bar{p}}_{2E}/(Br_0^2), \tag{A 6}$$

$$\sigma_{30}=\frac{[(r_0^{-1}-2n^2r_0^{-3}\Lambda)\mathscr{F}_1-2(\mathscr{F}+\delta_{01}r_0^{-1}\partial_\theta)]\,\mathrm{i}n\bar{\bar{p}}_{2E}}{2Br_0}+\frac{(\delta_{01}+\delta_0r_0^{-1})\Lambda\bar{\bar{p}}_{2E}}{B}, \tag{A 7}$$

$$t_{5E}=[q_{30}-\mathscr{F}_1A_{2E}-(\mathrm{i}\alpha_0\sigma_3x_1+r_0^{-1}(\delta_{01}+\delta_0r_0^{-1})\partial_\theta)\bar{\bar{v}}_{2E}-\mathrm{i}\alpha_0\partial_{x_1}\bar{\bar{p}}_{2E}]/B, \tag{A 8}$$

$$B_{4E}=-[2n^2Br_0^{-3}\Lambda^{-1}A_{2E}+6\mathrm{i}\alpha_0\Gamma_3\bar{\bar{v}}_{2E}+(\Lambda^2+\tfrac{1}{2}n^2r_0^{-4}-3n^4r_0^{-6}\Lambda^{-1})\bar{\bar{p}}_{2E}]/B \tag{A 9}$$

where, in (A 7), $\mathscr{F}=\mathrm{i}\alpha_0\sigma_3x_1+\Gamma_1\partial_{x_1}-\delta_0r_0^{-2}\partial_\theta$, and $\mathscr{F}_1$ is defined below (4.17).

The expression for χ in (4.40) is

$$\chi = -6\left(\frac{\Gamma_3}{\Gamma_1}\right)\mathscr{F}_1\bar{\bar{v}}_{2E} + 2\mathrm{i}\alpha_0\sigma_4 x_1\bar{\bar{v}}_{2E} + \frac{(n^4\Lambda^{-1} - \frac{3}{2}n^2r_0^2)\mathscr{F}_1\bar{\bar{p}}_{2E}}{Br_0^6}$$
$$+ \frac{\mathrm{i}\alpha_0\sigma_3 x_1(2n^2 - \Lambda r_0^2)\bar{\bar{p}}_{2E}}{Br_0^3} + \frac{4\mathrm{i}n^2\alpha_0\partial_{x_1}\bar{\bar{p}}_{2E}}{r_0^3\Lambda}$$
$$+ \frac{[r_0^{-4}\delta_0(10n^2 - 9r_0^2\Lambda) + r_0^{-3}\delta_{01}(2n^2 + r_0^2\Lambda) + 2\Lambda\delta_{02}]\partial_\theta\bar{\bar{p}}_{2E}}{Br_0} - 2\delta_0 r_0^{-2}\partial_\theta A_{2E}. \quad \text{(A 10)}$$

This expression for χ may be compared with the right-hand side of (B 7) of SBB for which the swirl was zero so that $\delta_0 = \delta_{01} = \delta_{02} = 0$. To make the identification we also let $r_0 \to \infty$ in (A 10) keeping n^2/r_0^2 fixed, in which case (A 10) reduces to the two (first) terms involving $\bar{\bar{v}}_{2E}$ and $\mathscr{F}_1$ becomes $c_0\partial_{x_1} + \mathrm{i}\alpha_0 c_2 x_1$. In the present theory it was not considered necessary to carry the term $\mathrm{i}\alpha_2 c_0 x_1$ in this operator although it was retained in SBB where in addition it was assumed that $\alpha_2 c_0 + \alpha_0 c_2 = 0$ so that the perturbations had a prescribed real frequency. Also, in SBB it was assumed that $\sigma_4 = 0$, as the initial aim was to construct a theory that would match downstream to that of Hall & Smith (1991), although as explained in Part 1, this assumption may easily be dropped. Hence in the situation considered in SBB, χ in (A 10) reduces to

$$\chi = -6c_0\Gamma_3\Gamma_1^{-1}\partial_{x_1}\bar{\bar{v}}_{2E}, \quad \text{(A 11)}$$

which is the right-hand side of (B 7) of SBB (when divided by $\mathrm{i}\alpha_0$ to relate $\bar{\bar{Q}}_{5E}$ to $\bar{\bar{u}}_{5E}$) when the relations $\Gamma_1 = b_1$ and $6\Gamma_3 = b_3$ are noted.

REFERENCES

BATCHELOR, G. K. & GILL, A. E. 1962 Analysis of the stability of axisymmetric jets. *J. Fluid Mech.* **14**, 529–551.

BROWN, S. N., LEIBOVICH, S. & YANG, Z. 1990 On the linear instability of the Hall-Stewartson vortex. *Theor. Comput. Fluid Dyn.* **2**, 27–46.

BROWN, S. N. & SMITH, F. T. 1996 On vortex/wave interactions. Part 1. Non-symmetrical input and cross-flow in boundary layers. *J. Fluid Mech.* **307**, 101–133.

BURGGRAF, O. R. & FOSTER, M. R. 1977 Continuation or breakdown in tornado-like vortices. *J. Fluid Mech.* **80**, 685–703.

CHURILOV, S. M. & SHUKHMAN, I. G. 1994 Nonlinear spatial evolution of helical disturbances to an axial jet. *J. Fluid Mech.* **281**, 371–402.

DAVIS, D. A. R. & SMITH, F. T. 1994 Influence of cross-flow on nonlinear Tollmien–Schlichting/vortex interaction. *Proc. R. Soc. Lond.* A **446**, 319–340.

DUCK, P. W. 1986 The inviscid stability of swirling flows: large wavenumber disturbances. *Z. Angew. Math. Phys.* **37**, 340–360.

FOSTER, M. R. & SMITH, F. T. 1988 Stability of Long's vortex at large flow force. *J. Fluid Mech.* **206**, 405–432.

HALL, P. & SMITH, F. T. 1991 On strongly nonlinear vortex/wave interactions in boundary-layer transition. *J. Fluid Mech.* **227**, 641–666.

LEIBOVICH, S. & STEWARTSON, K. 1983 A sufficient condition for instability of columnar vortices. *J. Fluid Mech.* **126**, 335–356.

SMITH, F. T., BROWN, S. N. & BROWN, P. G. 1993 Initiation of three-dimensional nonlinear transition paths from an inflexional profile. *Eur. J. Mech.* B **12**, 447–473 (referred to herein as SBB).